ANALYSIS OF THE KINETICS OF THE SOLIDIFICATION OF STEEL FORGING INGOTS OF DIFFERENT CONFIGURATIONS. PART II. RESULTS FROM COMPUTER MODELING[*]

A. N. Romashkin, V. S. Dub, D. S. Tolstykh,
A. N. Mal'ginov, I. A. Ivanov, and G. A. Ekhvaya

UDC 669-412

Results are presented from the use of computer modeling to study the effect of the configuration of forging ingots on the kinetics of their solidification. Aspects of the change in solidification rate in the vertical and horizontal directions over the ingot cross section are discussed, and calculations are performed to determine the solidification coefficients of steels as they harden in steel ingot molds. The results obtained by computer modeling are compared with results obtained by cold modeling.

Keywords: *solidification, kinetics, ingot, computer modeling.*

The computer modeling of the operations performed in a manufacturing cycle is an efficient and promising method of reducing the amount of financial resources and time spent in the fabrication of metal products. Such an approach makes it possible to find the values of the process parameters which are optimum from the standpoint of ensuring that the prescribed quality characteristics of the metal are reproduced over a narrower range of values. That in turn makes it possible to elevate the level of the properties of the final product's metal while also reducing their scatter [1].

With a satisfactory degree of accuracy, computer modeling of the process of making ingots can reveal the effects of the main process parameters – the configuration of the casting equipment and the temperature-rate regimes of the casting operation – on the quality characteristics of the ingots. Then this information can be used to optimize the technology chosen to obtain the ingots. Presented below are results from the use of this approach to evaluate the effect of the configuration of the ingots on the kinetics of their solidification. This effect is the factor that in large part determines the ingots' chemical inhomogeneity and the associated structural nonuniformity.

Method. Ingot solidification was examined by computer modeling with the use of the Large Ingot program, which is designed for steel forging ingots. The ingots in the study were similar in configuration to the ingots examined by cold modeling (see Part 1). We studied nine configurations of ingots weighing 360 tons (Fig. 1): the ratio $H/D = 1.0, 1.5, 2.0$. The conicity $K = 2\%, 10\%, 18\%$.

The following initial data were used to model the solidification of ingots of different geometries:

1) the grade of steel that was cast was 15KhN2MFA (Table 1);

2) the casting equipment was made of steel 35L;

3) the hot top was kept heated with the use of asbestos panels 0.010 m thick, one course of grade-Sh1 fireclay brick 0.065 m thick, and a heat-insulating ProFax insert 0.065 m thick;

4) the surface of the metal was covered by the heat-insulating mixture Nermat (in a layer 0.010 m thick) for 10 min after all of the metal was poured into the mold;

---

[*] For Part 1 see *Metallurgist*, No. 11, 1040–1052 (2016).

$K = 2\%$

$K = 10\%$

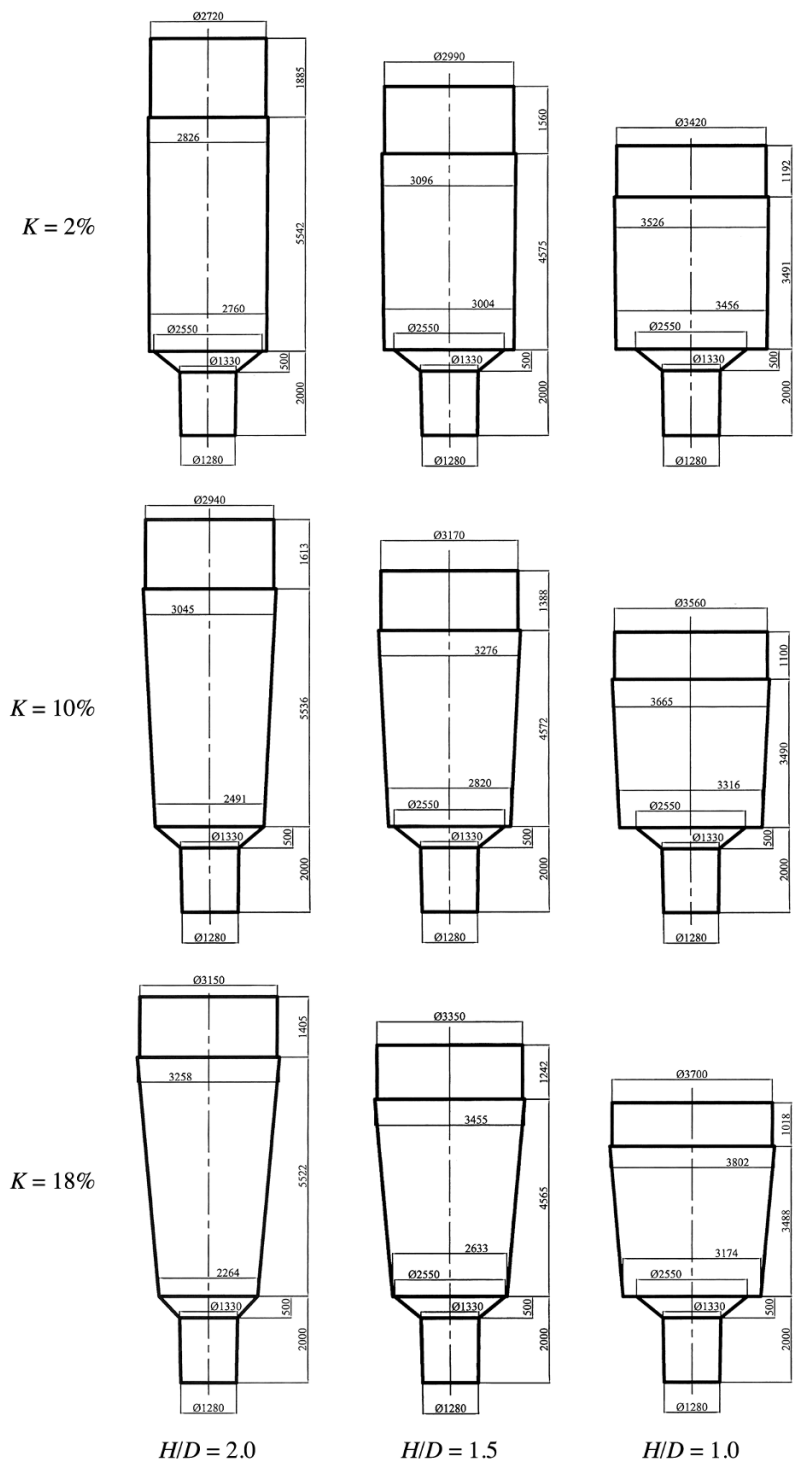$K = 18\%$

$H/D = 2.0$ $H/D = 1.5$ $H/D = 1.0$

Fig. 1. Dimensions of the 360-ton ingots that were studied.

5) casting time – 38 min – was determined based on the formula proposed in [3] for calculating the weight-based casting speed:

$$v_{cast} = 0.5M^{1/2} \tag{1}$$

(v_{cast} is the rate at which the mold is filled, tons/min; M is the weight of the ingot, tons);

1164

TABLE 1. Grade-Stipulated Chemical Composition and Actual Chemical Composition of Steel 15Kh2NMFA (min/max)

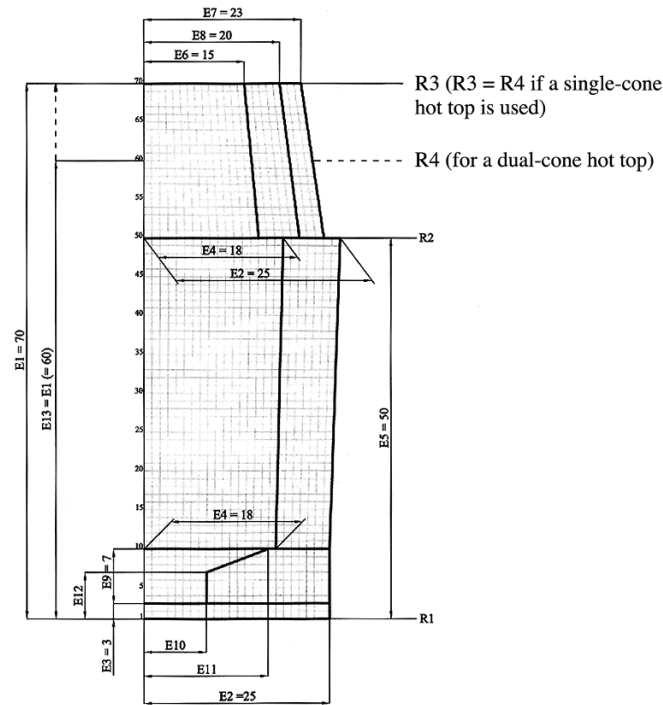| Content of the elements, wt. %										
C	Si	Mn	Cr	Ni	S	P	Mo	V	Cu	Al
TU 0893-013-00212179-2003										
0.13/0.18	0.17/0.37	0.3/0.6	1.8/2.3	1.1/1.5	–/0.020	–/0.020	0.5/0.7	0.10/0.12	0.00/0.30	–/0.008
Actual										
0.15	0.27	0.5	2.1	1.3	0.005	0.007	0.6	0.11	0.01	0.008

Fig. 2. Scheme used to subdivide the ingot into volumes/blocks.

6) the temperature of the metal before casting was 1610°C;

7) the temperature of the casting equipment: ingot mold – 100°C; hot top – 150°C; bottom plate – 200°C.

The cylindrical hot-top part of the ingot comprised a constant 20% of the ingot's total weight. Here, the diameter of the bottom of the hot top was 100 mm less than the diameter of the top of the ingot.

The convex part of all the ingots had the form of a truncated cone with the following dimensions: height 1.5 m; bottom diameter 1.28 m; top diameter 1.33 m. The solidification of the ingots was modeled with allowance for the formation of their solid skin during the casting operation.

The values calculated for the liquidus and solidus temperatures of the ingots in accordance with their prescribed chemical composition were 1515 and 1470°C, respectively.

The algorithm that was created to calculate the dynamics of ingot cooling and was incorporated into the Coarse Ingot program is based on the solution of the differential heat-conduction equation

$$\rho C \frac{\partial T}{\partial \tau} = \text{div}(\lambda \text{grad}(T)) q_V,$$ (2)

TABLE 2. Heat Capacity and Thermal Conductivity of the Materials Used in Computer Modeling of the Solidification of Forging Ingots

Characteristics of the materials	Properties at different temperatures, °C								
	200	300	400	500	600	700	800	1000	1400
Steel 35L (the material of the casting equipment)									
λ, W/(m·K)	0.71	0.66	0.58	0.59	0.6	0.65	0.66	0.79	1.06
C_p, J/(kg·K)	820	860	910	1010	1080	1090	1080	1160	1210
Asbestos									
λ, W/(m·K)	0.168	0.19	0.216	0.240	0.264	0.288	0.312	0.360	0.456
C_p, J/(kg·K)	1128	1197	1253	1303	1374	1402	1461	1520	1679
Grade Sh1 fireclay									
λ, W/(m·K)	1.05	1.08	1.12	1.16	1.19	1.25	1.26	1.34	1.48
C_p, J/(kg·K)	212	220	228	235	241	247	251	256	261
ProFax									
λ, W/(m·K)	0.12	0.14	0.16	0.19	0.22	0.24	0.26	0.48	0.60
C_p, J/(kg·K)	901	982	1063	1120	1152	1168	1175	1205	1289
Thermal insulation for the hot-top part (equivalent value)									
λ. Вт/(м·K)	0.347	0.40	0.457	0.512	0.567	0.622	0.677	0.787	1.007
C_p, J/(kg·K)	1.287	1.34	1.389	1.434	1.475	1.512	1.545	1.599	1.659
Heat-insulating covering for the surface of the metal in the hot top									
λ, W/(m·K)	0.114	0.14	0.172	0.201	0.230	0.259	0.288	0.346	0.360
C_p, J/(kg·K)	614	697	741	773	800	826	850	896	987
Steel 15KhN2MFA (the steel being cast)									
λ, W/(m·K)	37.9	36.8	36.8	24.5	32.4	28	27.2	27.7	27.7
C_p, J/(kg·K)	511	523	536	544	553	561	569	582	590

where q_V is the heat of crystallization (determined with $T = [T_L; T_S]$), W/m³; T is temperature, K; ρ is density, kg/m³; λ is thermal conductivity, W/(m·K); C is heat capacity, J/(kg·K); and τ is time, sec.

It was assumed that the density of steel 15Kh2NMFA is 7.1 tons/m³ in the semi-solid state and 7.8 tons/m³ in the solid state.

The impurity redistribution was calculated by using a model of equilibrium crystallization. In accordance with this model, the percentage of the liquid phase in a cell (η_L) and the impurity concentration in it ($CL_{(i)}$) can be calculated from the expressions

$$\eta_L = (C_{(i)} - CS_{(i)})/(CL_{(i)} - C_{(i)});\qquad(3)$$

$$CL_{(i)} = C_{(i)}/(1 + (k-1)\eta_S),\qquad(4)$$

where $C_{(i)}$, $CS_{(i)}$, and $CL_{(i)}$ are the initial concentration of the *i*th impurity, the running concentration of this impurity in the solid phase, and the running concentration of this impurity in the liquid phase, %; k is the distribution coefficient, frac. un.; and η_L and η_S are, respectively, the relative contents of the liquid phase and the solid phase, frac. un.
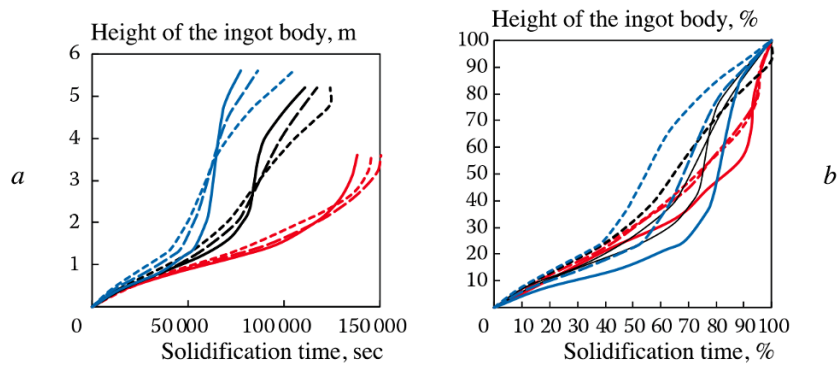
Fig. 3. Kinetics of vertical solidification of the axial part of 360-ton ingots in absolute (*a*) and relative (*b*) coordinates: ──) $K = 2\%$; ─ ─ ─) $K = 10\%$; ·· ·) $K = 18\%$; blue lines – $H/D = 2$; black lines – $H/D = 1.5$; red lines $H/D = 1$.
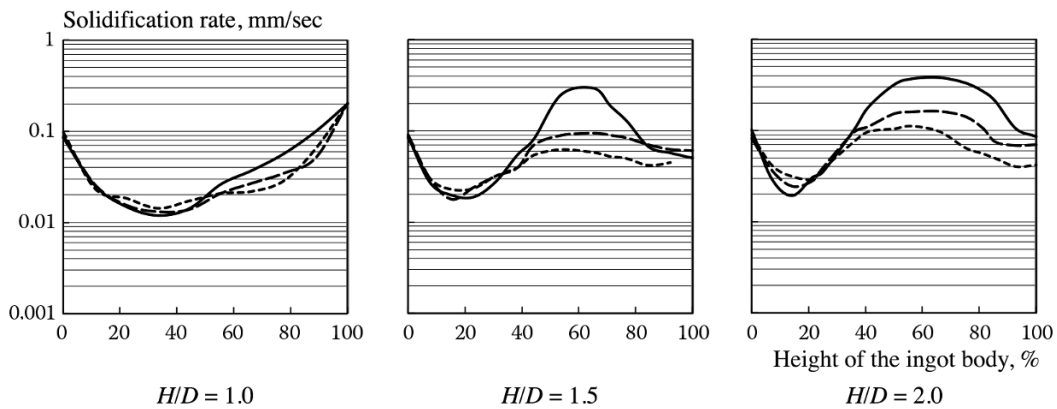

Fig. 4. Change in the vertical rate of crystallization in ingots studied by cold modeling: ──) $K = 2\%$; ─ ─ ─) $K = 10\%$; ·· ·) $K = 18\%$ (the data are for 360-ton ingots of steel 15Kh2NMFA having different configurations).
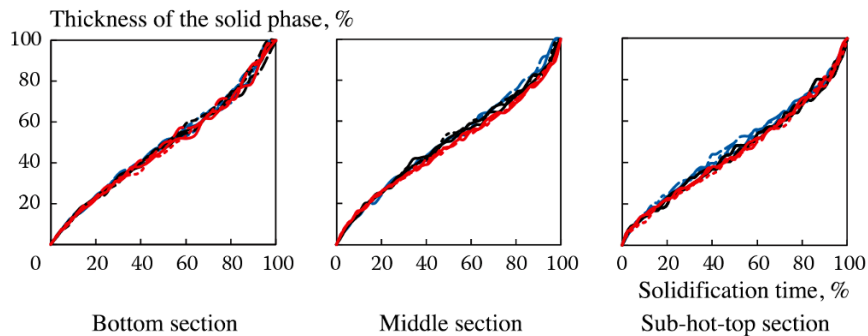

Fig. 5. Change in the thickness of the solid phase in the horizontal direction for 360-ton ingots of different configurations: ──) $K = 2\%$; ─ ─ ─) $K = 10\%$; ·· ·) $K = 18\%$; blue lines – $H/D = 2$; black lines – $H/D = 1.5$; red lines – $H/D = 1$.

Shrinkage is calculated based on the use of the volumetric shrinkage coefficient, which characterizes the relative change in the volume of the metal (during cooling/heating) for each 1°C change in temperature. The amounts of shrinkage that the steel undergoes during cooling of the liquid metal, during the conversion from the liquid state to the solid state, and
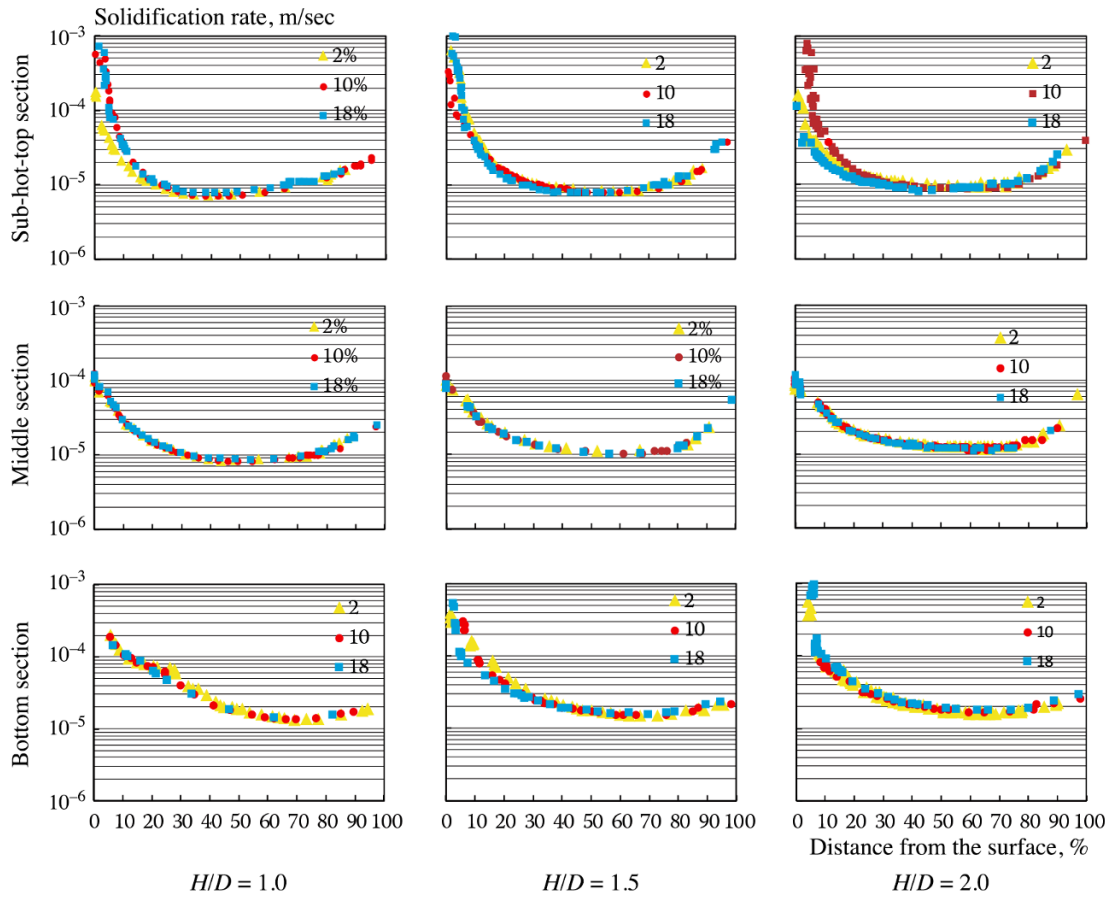
Fig. 6. Dependence of the rate of growth of the solid phase in the horizontal direction on relative radial position in the sub-hot-top section, midsection, and bottom section of the ingot.

during cooling of the solid phase are characterized by the volumetric shrinkage coefficients α_L, α_{L-S}, and α_S. The specific value of the coefficients α_L and α_{L-S} depends on the composition of the steel. To perform calculations, we took 0.010%/K as the steel's volumetric shrinkage coefficient in the liquid state and 0.006%/K as the value of this coefficient in the solid state.

The following formula was used to calculate the amount by which the volume of metal in a unit cell at a temperature above the liquidus temperature changes during the time $\Delta\tau$:

$$\Delta V_\Sigma = \Delta V_L = V_{\tau-\Delta\tau} - V_{\tau-\Delta\tau}\, \alpha(T_{\tau-\Delta\tau} + T_\tau), \tag{5}$$

where ΔV_Σ is the total amount of shrinkage of the metal of the cell due to its cooling during the time $\Delta\tau$, m^3; ΔV_L is the shrinkage of the liquid phase of the cell due to its cooling during the time $\Delta\tau$, m^3; $V_{\tau-\Delta\tau}$ is the volume of the liquid phase in the cell at the previous moment of time, m^3; α is the volumetric shrinkage coefficient of the metal, frac. un./K; and $T_{\tau-\Delta\tau}$ and T_τ are the temperatures of the cell at the previous and current moments of time, °C.

Before performing calculations, the Coarse Ingot program divides the thermal system being studied into elementary volumes/blocks in accordance with the symmetry of the problem (Fig. 2). In the case of a cylindrical ingot, there is no heat exchange in the direction of the angular coordinate. The nodal points at which temperatures are calculated are at the corners of the elements of the subdivision. The distributed thermal constraints which exist in an actual body are replaced by discrete values of thermal conductivity between the nodal points.

Table 2 shows values of the thermophysical properties of the materials of the casting equipment and the steel being cast.

Results of determination of vertical solidification rate in the computer modeling. Figure 3 shows the results obtained from determining the thickness of the solid phase in the vertical direction.

The results obtained from computer modeling of the ingots that were examined confirm the conclusions made in the cold modeling. In particular, it was shown that the curve which describes the dependence of the rate of growth of the solid phase on the position in the ingot relative to the vertical axis is S-shaped in character (Fig. 4). The position of the point where the horizontally directed solidification fronts meet one another (the height to which the effect of the bottom plate extends) – which corresponds to the lowest solidification rate – is equal to roughly $0.32H$ when $H/D = 1.0$; $0.20H$ when $H/D = 1.5$; $0.15H$ when $H/D = 2.0$ (see Fig. 4).

Accordingly, the value of the coefficient in Eq. (6), obtained by cold modeling, is equal to 0.3, i.e., the results obtained by computer modeling indicate that the vertical solidification rate is 0.6 of the horizontal rate (explanations for this finding were given in the first part of this article):

$$h_{\text{rel}} = \xi/(H/D), \tag{6}$$

where h_{rel} is the length of the zone affected by the bottom plate, frac. un.; ζ is a coefficient, which in the given case has a value of 0.40.

An analysis of the graphs in Fig. 4 which describe the change in vertical solidification rate over the height of the axial part of the ingot shows that in ingots with $H/D = 1$ there is no decrease in the rate of solidification during its final stages; from the moment solidification rate reaches its lowest value in the bottom part of the ingot, the rate uniformly increases until the ingot has completely solidified. This pattern is probably related to the weak heating effect of the hot top of such ingots due to the rapid cooling that they undergo. To keep the relative weight of the metal in the hot top constant for the type of ingots being discussed, the height of the hot top is decreased and its diameter is increased as the value of H/D decreases. Thus, the diameter of the hot top is maximal for ingots of the given type ($H/D = 1$). This accounts for the maximal area of the surface of the metal, which is characterized by the highest capacity for heat removal. The situation just described led to relatively rapid cooling of the hot top and a decrease in its heat content. The reduced heat content in turn resulted in less heating of the layers of metal under the hot top, so that there was no decrease in the rate of solidification of the metal in the body of the ingot. The fact that this rate did not decrease is reflected in the similar path of the curve which shows the kinetics of the ingot's solidification. Thus, when there is a decrease in the value of H/D for ingots, it is necessary to increase the relative amount of metal in the hot top in order the maintain the conditions necessary for the provision of molten metal to the solidifying ingot. This conclusion is supported by English and American practice in the casting of large ingots [4], whereby the volume of the hot top is calculated based not on the weight of the ingot but on the cross-sectional area of its upper part [5, 6]. The calculation is performed by using Eq. (7):

$$V_{\text{ht}} = 0.4585 \cdot D^{2.7}, \tag{7}$$

where V_{ht} is the volume of the hot top, m^3; D is the upper diameter of the body of the ingot, m.

Compared to the cold modeling, the computer modeling made it possible to more accurately evaluate the effect of conicity on the kinetics of solidification: the results confirmed the thesis advanced in Part I of this article to the effect that the maximum solidification rate increases as the conicity of the ingot approaches zero (see Fig. 4).

It is evident from the data in Fig. 4 that an increase in H/D is accompanied by expansion of the range of the rate of solidification over the height of the axial part of the ingot. The overall level of solidification rate remains high in this case, which is indicative of favorable (in regard to keeping the ingot metal from becoming chemically inhomogeneous) conditions for the solidification of an ingot with a high value of H/D: a high solidification rate slows the development of segregation processes and thus helps make the ingot metal more chemically homogeneous.

The results from determination of the solidification rate of ingots in the horizontal direction by computer modeling are shown in Fig. 5. Figure 6 shows values of solidification rate in this direction for all of the ingot configurations that were considered.

It is apparent from the relations in Figs. 6 and 7 that the configuration of the ingot does affect its rate of solidification in the horizontal direction. However, this effect is slight and is manifest mainly when there is a change in the parameter H/D.
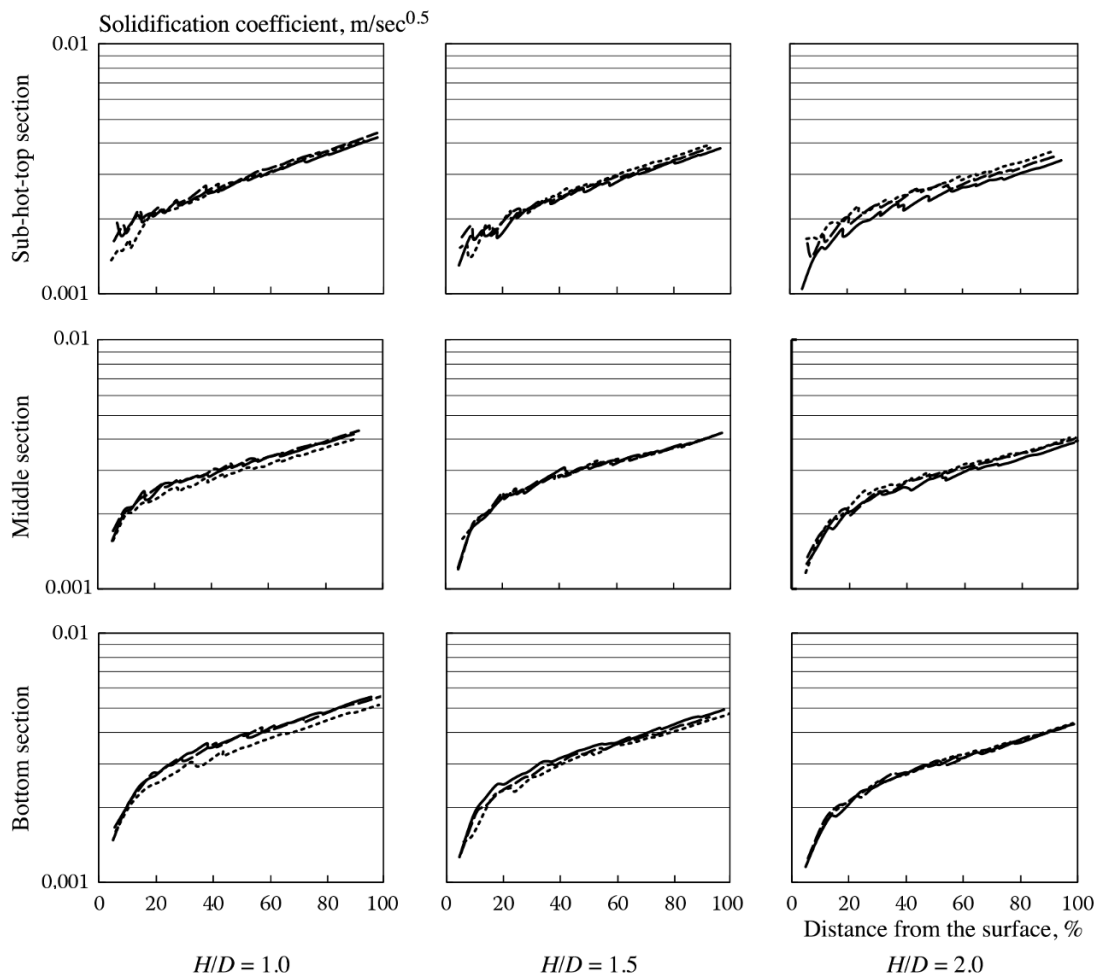
Fig. 7. Solidification coefficient for different sections of the ingot based on the results obtained by computer modeling: ——) $K = 2\%$; – – –) $K = 10\%$; · · ·) $K = 18\%$.

Conicity (K) has a significant effect only in the region of the ingot underneath the hot top. The lowest values of solidification rate in the horizontal direction are shifted closer to the surface with an increase in the ingot's height: for example, whereas the lowest solidification rate in the bottom part of the ingot is seen at a level which is 70% removed from the surface, the corresponding level is at roughly 50% in the ingot's midsection and at 35% in the region under the hot top.

Solidification takes place most rapidly in the bottom region of the ingot. For all the ingot configurations that were examined, solidification rate decreased with decreasing distance to the hot top. Accordingly, the rate of solidification is lowest in the sub-hot-top region of the ingot. Here, the absolute value of the lowest solidification rate (characteristic of the region just mentioned) depends on the value of H/D: it is roughly 0.006 mm/sec in ingots with $H/D = 1.0$; 0.007 mm/sec in ingots with $H/D = 1.5$; 0.009 mm/sec in ingots with $H/D = 2.0$. In other words, as noted above an increase in H/D is accompanied by an increase in the overall rate of solidification of ingots.

A comparison of the horizontal solidification rates obtained by cold modeling and the corresponding rates obtained by computer modeling shows that the steel solidifies roughly 10 times faster than sodium hyposulfite: the average value of the solidification rate over approximately 90% of the radius of the steel ingot in its midsection varies within the range $(8–20) \cdot 10^{-5}$ m/sec; the hyposulfite solidifies at a rate in the range $(2–10) \cdot 10^{-6}$ m/sec in the same middle section of the ingot.

This confirms the conclusion that was reached in Part I of this article from a comparison of values of the similarity criterion SL for these two liquids.

1170

Figure 7 shows graphs that describe the change in the solidification coefficient of steel over the radius of the test ingots at three levels: in the bottom part of the ingot, in its midsection, and under the hot top. It can be seen that the coefficient varies at all three levels. However, its change is relatively small and its absolute value is approximately 3 ± 1 mm/sec$^{0.5}$ (23 ± 8 mm/min$^{0.5}$). This value is fully consistent with the available literature data [7, 8]. Comparison of the values obtained for the solidification coefficient by computer modeling and the value found for this parameter in sodium hyposulfite by cold modeling confirms the conclusion reached previously (in comparing the horizontal solidification rates for these two liquids) that the steel solidifies about 10 times faster than sodium hyposulfite: the average value of the solidification coefficient for the latter is roughly 0.4 mm/sec$^{0.5}$ (3 mm/min$^{0.5}$).

A change in the solidification coefficient that is less than half of an order of magnitude can be considered acceptable for an approximate evaluation of the time of solidification of ingots in relation to their transverse dimension. Accordingly, the values of this criterion that have been obtained in this investigation can be used in engineering practice to perform the corresponding calculations.

Thus, the results of the computer modeling are in agreement with the results obtained by cold modeling and the experimental data in [9–16] on the kinetics of solidification of steel forging ingots: the rate of solidification of such an ingot in the vertical direction initially decreases and then increases somewhat before decreasing again by the end of the solidification process. As for solidification in the horizontal direction, the curve which describes the change in solidification rate over the cross section of the ingot is U-shaped in character and has a minimum at the 60–70% level.

Conclusions. The results that have been obtained by studying the kinetics of the solidification of steel forging ingots on the basis of computer modeling permit the following conclusions:

1) the rate of solidification of the ingots increases with an increase in *H/D*;

2) ingot solidification rate is most affected by the value of the ratio *H/D*; the effect of conicity is negligible.

3) the curve which shows the dependence of the rate of solidification in the vertical direction on the height of the ingot is S-shaped in character and has a maximum at the 60–70% level; and

4) the curve which shows the dependence of the rate of solidification in the horizontal direction on the distance from the surface is U-shaped and has minima at the levels corresponding to distances of 50, 70, and 85% from the surface in the bottom of the ingot, its midsection, and the region under the hot top.

These conclusions are consistent with the conclusions reached in Part I of this investigation based on results obtained by cold modeling. On the whole, the results show that long ingots solidify faster than truncated ingots. In connection with this, longer ingots will be characterized by less chemical and structural nonuniformity because the extent to which such nonuniformity develops depends on solidification rate. Longer ingots should therefore be used to make products that have to meet stringent requirements on the uniformity of their properties. This applies in particular to large ingots.

REFERENCES

1. A. N. Romashkin, A. N. Mal'ginov, D. S. Tolstykh, et al., "Effect of the geometry of an ingot on the volume of axial porosity in it," *Komp. Issled. Modelir.*, **7**, No. 1, 107–113 (2015).
2. V. S. Dub, A. N. Romashkin, E. V. Makarycheva, et al., "Method of developing a technology for the production of forging ingots," *Tyazh. Mash.*, No. 7, 13–20 (2012).
3. V. S. Doub, A. N. Romashkin, and A. N. Mal'ginov, "Main trends in the development of technology for casting steel into ingots," *Metallurgist*, **57,** No. 5/6, 487–500 (2013).
4. "Steels for large forgings," *Les Aciers Fins et Speciaux Francais*, No. 25, 65–73 (1958).
5. A. D. MacMillan, "Report at the International Conference on Problems in Forging (Sheffield, England, 1967)," GPNTB Translation No. 68/84874.
6. G. A. Fischer, *Trans. ASTM*, **62**, 1137 (1962).
7. V. V. Nazaratin, *Technology of the Production of Steel Castings for Critical Applications*, Mashinostroenie, Moscow (2006).

8. V. V. Nazaratin, A. N. Romashkin, I. A. Ivanov, et al., "Method of designing forging ingots without axial defects," *Met. Mashinostr.*, No. 3, 40–52 (2010).

9. V. S. Dub, *Investigation of Non-Axial Segregation and the Development of Methods for Suppressing It in Large Ingots: Eng. Sci. Doct. Dissert.*, Moscow, TsNIITMASh (1980).

10. V. M. Senopal'nikov, G. A. Lubenets, and V. A. Sivkov, *Control of Processes in the Solidification of an Ingot of Killed Steel*, NGTU, N. Novgorod (2009).

11. G. S. Lozhkin, "Study of the effectiveness of accelerating the vertical crystallization of ingots to improve their quality," in: *Problems of the Steel Ingot. No. 6*, Metallurgiya, Moscow (1976), pp. 108–110.

12. V. A. Efimov, A. G. Tarapon, and B. V. Platanov, "Kinetics of the solidification of 13.1-ton slabbing ingots of killed steel," in: *Problems of the Steel Ingot. No. 5*, Metallurgiya, Moscow (1974), pp. 539–543.

13. S. Ya. Skoblo, "Formation of the structure of an ingot of killed steel," in: *Problems of the Steel Ingot. No. 3*, Metallurgiya, Moscow (1969), pp. 33–38.

14. W. Martin and E. Thon, *Stahl und Eisen*, **26**, 1765–1774 (1955).

15. G. D. Molonov, N. F. Sapelkin, and S. V. Leporskii, "Aspects of the crystallization of large slabbing ingots of killed steel," in: *Problems of the Steel Ingot. No. 6*, Metallurgiya, Moscow (1976), pp. 102–107.

16. Yu. G. Khorunzhii and V. L. Efimov, "On determining the vertical rate of solidification of a large forging ingot," in: *Problems of the Steel Ingot. No. 3*, Metallurgiya, Moscow (1969), pp. 67–70.